

Rock Glacier Outflows May Adversely Affect Lakes: Lessons from the Past and Present of Two Neighboring Water Bodies in a Crystalline-Rock Watershed

Boris P. Ilyashuk,^{*,†} Elena A. Ilyashuk,[†] Roland Psenner,[†] Richard Tessadri,[‡] and Karin A. Koinig[†]

[†]Institute of Ecology, University of Innsbruck, Technikerstraße 25, 6020 Innsbruck, Austria

[‡]Institute of Mineralogy and Petrography, University of Innsbruck, Innrain 52, 6020 Innsbruck, Austria

Supporting Information

ABSTRACT: Despite the fact that rock glaciers are one of the most common geomorphological expressions of mountain permafrost, the impacts of their solute fluxes on lakes still remain largely obscure. We examined water and sediment chemistry, and biota of two neighboring water bodies with and without a rock glacier in their catchments in the European Alps. Paleolimnological techniques were applied to track long-term temporal trends in the ecotoxicological state of the water bodies and to establish their baseline conditions. We show that the active rock glacier in the mineralized catchment of Lake Rasass (RAS) represents a potent source of acid rock drainage that results in enormous concentrations of metals in water, sediment, and biota of RAS. The incidence of morphological abnormalities in the RAS population of *Pseudodiamesa nivosa*, a chironomid midge, is as high as that recorded in chironomid populations inhabiting sites heavily contaminated by trace metals of anthropogenic origin. The incidence of morphological deformities in *P. nivosa* of ~70% persisted in RAS during the last 2.5 millennia and was ~40% in the early Holocene. The formation of RAS at the toe of the rock glacier most probably began at the onset of acidic drainage in the freshly deglaciated area. The present adverse conditions are not unprecedented in the lake's history and cannot be associated exclusively with enhanced thawing of the rock glacier in recent years.



INTRODUCTION

Perennially frozen and glacierized high-alpine areas react very sensitively to changes in air temperature and even small differences in temperature determine their frozen status. As a consequence, glaciers in the European Alps, for example, have lost 30–40% of surface area since the end of the Little Ice Age (~middle of 19th century),¹ and the lower permafrost limit is estimated to have risen by ~1 m per year.² Discharge from melting glaciers and thawing permafrost can be highly enriched in solutes due to prolonged interaction with fine-grained rocks and freshly exposed mineral surfaces.^{3–5} Solute outflows from catchments characterized by cryospheric features can cause serious changes in water chemistry downstream. A survey of remote high altitude lakes in the European Alps⁶ has provided strong evidence of a substantial increase in base cation and sulfate concentrations in lake water over the past few decades, especially in lakes from glaciated areas. The increase of solutes in lake water was attributed to an enhanced weathering resulting from climate warming.

Until now, very little research has examined how changes in the mountain cryosphere affect downstream water quality, including the threats to ecosystem health and human use.⁷ Recent studies that investigated water quality in alpine

watersheds draining mineralized areas with sulfide-bearing lithologies demonstrate that retreating glaciers⁸ and degrading permafrost⁹ may adversely affect downstream ecosystems receiving meltwater runoff. The exposure of fresh surfaces of sulfide-rich rocks to air and oxygenated water by retreating glaciers or degrading permafrost increases the oxidation of sulfide minerals, which is responsible for the generation of natural acid rock drainage (ARD). ARD typically produces acid-sulfate waters enriched in Fe, Al, Mn, and various trace elements such as Cu, Ni, Pb, Zn, and others.^{10,11} Concentration of the dissolved minor and trace elements in natural ARD systems generated by retreating glaciers or degrading permafrost can be comparable to ARD associated with mining activity.^{8,9} Some of the mobilized trace elements associated with ARD pose a potential hazard to environmental quality and human health.

Although ice loss in permafrost can be orders of magnitude slower than in a glacier, the total permafrost area usually

Received: January 14, 2014

Revised: May 7, 2014

Accepted: May 7, 2014

Published: May 7, 2014



Figure 1. Map showing the location of the study site (a) and photograph of Lake Rasass (RAS) and the adjacent pond (RPD) and their catchments (b). The red arrows indicate the boundary of the active rock glacier. The map of Italy is reproduced from <http://d-maps.com/>.

exceeds the glacier-covered area in mountain environments and can contribute substantially to the hydrology of alpine catchments.¹² For example, the perennially frozen area in the European Alps is approximately three times larger than the glacier-covered area.¹³ Despite the fact that rock glaciers are one of the most common geomorphological expressions of mountain permafrost,^{14,15} still little is known about the geochemical content, especially about the trace-element composition of supra- and subpermafrost meltwater that drains rock glaciers.¹⁶ Until recently, most of the research conducted on rock glaciers primarily focused on their movement, origin, internal structure, and hydrology.^{4,14} However, the impacts of rock glacier solute fluxes on lakes downstream still remain largely obscure⁷ even though more than half of the world population relies on fresh water from mountain areas.¹⁷

Unexpected high nickel and manganese concentrations exceeding the appropriate EU limits for drinking water by more than an order of magnitude have recently been reported in a study investigating temporal trends in water chemistry of a remote high-mountain lake, Lake Rasass, situated at the toe of an active rock glacier the European Alps, Italy.¹⁸ The high concentrations of Mn and Ni were observed in the lake water enriched in sulfates (more than $4400 \mu\text{equiv}\cdot\text{L}^{-1}$). In contrast, negligible concentrations of these metals were recorded in the adjacent pond without a rock glacier in the catchment.¹⁸ In an earlier study, application of paleoecological techniques provided strong evidence of acidic conditions in Lake Rasass ($\text{pH } 5.8\text{--}6.5$) during at least the past two centuries.¹⁹ The overall results of the previous studies focused on the lake give evidence of naturally occurring ARD generated by the rock glacier in the Lake Rasass catchment.

The present study aims to explore the effects of rock glacier solute fluxes on a high alpine lake within a crystalline-rock watershed. We applied comparative research design in the study of two neighboring water bodies, Lake Rasass and the adjacent pond, with and without a rock glacier in their mineralized catchments having similar soil conditions and underlying geology. In addition, we used chironomid-based paleolimnological techniques to track long-term temporal trends in the ecotoxicological state of both water bodies and to establish their baseline conditions.

MATERIAL AND METHODS

Study Area. Lake Rasass (RAS; surface area = 1.5 ha, max. depth = 9.3 m) and the adjacent pond (RPD; surface area = 0.08 ha, max. depth = 1.6 m) are remote, fishless water bodies situated just 50 m away from each other, above the actual and historical timberline in the upper Vinschgau valley (2682 m a.s.l.) in the Central Eastern Alps, Italy (Figure 1). The bedrock geology of the valley belongs to the Austroalpine Ötztal-Stubai

crystalline complex,²⁰ and the average mineral composition of the bedrock is quartz (50%), feldspar (27%), muscovite (15%), chlorite (6%), and dolomite (2%).²¹ The chemical composition of the bedrock is characterized by sources of disseminated water-soluble sulfate ($\sim 180 \mu\text{g g}^{-1}$ dry weight (DW); total sulfur is $\sim 590 \mu\text{g g}^{-1}$ DW) and metals, including trace elements Mn ($\sim 597 \mu\text{g g}^{-1}$ DW), Ni ($\sim 24 \mu\text{g g}^{-1}$ DW) and Zn ($\sim 90 \mu\text{g g}^{-1}$ DW).²¹ The concentrations of Mn and Zn are comparable with their Earth crustal abundances,²² while Ni content is more than three times lower. Soil cover is sparse and bedrock is exposed in $\sim 80\%$ of the RAS and RPD catchment areas. The active rock glacier extends on a north-facing slope down to the shore of RAS and occupies $\sim 18.5\%$ of its catchment area which adjoins the permafrost-free catchment of RPD. Both water bodies lacking inflow streams have well-developed outflows. Near the RPD shoreline, there are visible sources of groundwater that infiltrates onshore discharges. Since the rock glacier is located only a few meters upslope from RAS, its internal drainage system, a common feature of rock glaciers,^{4,23,24} is most likely connected to the lake, and meltwater seeps from the rock glacier into RAS through cracks and fractures in the bedrock.

Since 1980, summer and cold-season (October–May) temperatures in the European Alps show a simultaneous, strong increase, which is unprecedented over the last millennium.²⁵ A multifold increase in concentrations of the dominant ions (Mg^{2+} , SO_4^{2-} , and Ca^{2+}) and electrical conductivity in the RAS water over the last two decades (1986–2005), recorded by Thies et al.,¹⁸ may reflect current permafrost degradation in the rock glacier under the recent warming. Monnier and Kinnard²⁶ assume that indications of degrading permafrost in a rock glacier may also be the near-melting-point (0°C) thermal regime of permafrost year-round and a high water content ($>40\%$) in deeper parts of a rock glacier. As solutes concentrate and the freezing point decreases during fluid freezing,²⁷ it is most likely that highly concentrated salt solutions seep from the rock glacier into RAS through the cold season.

Water Chemistry. Both water bodies were sampled for limnochemical analyses at least twice during the open-water seasons of 2010–2012. Water samples were taken with a Patalas-Schindler sampler (UWITEC, Austria) at 2-m intervals along a vertical profile in RAS and from 0.5 m water depth in the shallower RPD. The physicochemical parameters of water, such as conductivity, pH, alkalinity, and concentrations of major ions and nutrients were determined following standard methods and analytical quality control procedures as described in Mosello and Wathne.²⁸ Metals (Ag, Al, As, Ba, Be, Cd, Co, Cr, Cu, Fe, Mn, Ni, Pb, Sr, Ti, V, Zn) in water samples were

assayed by inductively coupled plasma-optical emission spectrometry (ICP-OES) with standard addition methods.²⁹

Sediments and Biota: Sampling Strategy and Chemical Analyses. Sampling strategy was designed to compare metal concentrations in surface sediments and biota of the water bodies as follows: the RAS and RPD shallow waters against the RAS deep water, and between shallow waters of RAS and RPD. To provide background information for the sampling in the relatively deep RAS, bathymetric distribution and substratum associations of the most abundant macroinvertebrates were studied in the lake along a depth transect (Supporting Information (SI), Figure S1). Twenty macroinvertebrate samples were collected with an Ekman grab sampler (in deep water) and a kick net (in the upper littoral) at 0.5–1.0 m depth intervals along the east–west transect across the deepest point in the lake. Surface sediment (0–1 cm) samples were collected using an Ekman grab sampler with a lining of plastic inside from three random sites in shallow waters (0.5–1.5 m depth) of both water bodies and in deep water (6–8 m depth) of RAS. The sediment and biota sampling for subsequent multielement analysis was conducted in the early open-water season of 2012.

For multielement analysis of body tissues of aquatic organisms, larvae of the chironomid midge *Pseudodiames nivosa* (Diptera: Chironomidae), the oligochaete *Tubifex tubifex* (Oligochaeta: Tubificidae), and the aquatic moss *Warnstorffia exannulata* (Hypnales: Amblystegiaceae) were collected with a biological bottom dredge (EEF & GB Nets, UK) in the RAS deep-water habitats (6–8 m depth). Larvae of the chironomid *P. nivosa* were also collected in RPD (0.5–1.5 m depth). The predatory aquatic beetle *Agabus bipustulatus* (Coleoptera: Dytiscidae) was collected with a kick net in shallow-water habitats (0.5–1.5 m depth) of both water bodies. Invertebrates were held in lake water at field temperatures for transport to the laboratory where they were sorted according to species, cleaned with distilled water, placed in Petri dishes and kept at 4 °C for 24 h in order to purge the guts. Thereafter they, as well as the aquatic moss *W. exannulata*, were rinsed with distilled water and frozen pending analyses. Only plastic storage vessels and tools (tweezers, scapulae, etc.) were used. All plastic labware was soaked in 1% nitric acid for at least 24 h and rinsed with doubly deionized water to leach out metal ions.³⁰

All sediment and biota samples were dried in an oven at 25 °C to a constant weight (3–4 days) and homogenized with an agate mortar and pestle, and triplicate 0.5 g aliquots of every sample were used for the analysis. The samples were dissolved with concentrated nitric acid³¹ using the microwave digestion technique.³² A total of 42 elements (Ag, Al, As, Ba, Bi, Br, Ca, Cd, Cl, Cr, Cu, Fe, Ga, Ge, Hf, I, K, Mg, Mn, Mo, Na, Nb, Ni, P, Pb, Rb, S, Sb, Se, Si, Sn, Sr, Ta, Th, Ti, Tl, U, V, W, Y, Zn, Zr) were assayed by energy dispersive X-ray fluorescence (EDXRF) analysis using calibration models based on fundamental parameter methods. In the sediment samples, ten major elements, Si, Al, Fe, Mn, Mg, Na, Ca, K, Ti, and P, were measured as their oxides. Analytical accuracy was verified by the use of CCRMP (Canadian Certified Reference Materials Project) reference samples. Recoveries were within 10% of the certified values.

Sediment Coring, Dating, and Chronology. Sediment cores were taken using UWITEC gravity and piston corers (UWITEC, Austria) in the deepest point of both water bodies in the summer of 2011. The 119.2 cm long sediment sequence from RAS was sectioned contiguously into 156 samples: at

0.22–0.50 cm resolution within the top 24 cm and at 1 cm resolution from 24 cm to the bottom. The 15.5 cm long sediment sequence from RPD was sectioned contiguously every 0.5 cm, resulting in a total of 31 samples. Chronological control for the sediment sequences was provided by accelerator mass spectrometry (AMS) radiocarbon dates derived from terrestrial plant macrofossils: six AMS ¹⁴C dates from the RAS sequence and four dates from the RPD sequence. The Bayesian statistical method of the OxCal software package version 4.2.1³³ was used to produce age-depth models (SI Figure S2). According to these estimates, the RAS and RPD sediment cores span time periods of ~10 200 years and ~3200 years, respectively. The ages are expressed in calibrated years before present (cal yr BP = calibrated years before AD 1950) (see SI 1 for further details).

Chironomid Analysis. Incidence of mouthpart abnormalities in chironomid larvae was used as measures of toxic stress in the water bodies. Occurrence of mouthpart deformities in chironomids is a sublethal effect of larval exposure to environmental stress factors.³⁴ Since mouthpart deformities may also be induced by toxic elements and their compounds not included in routine chemical analyses, they may better reflect environmental quality than chemical analysis alone. Assessment of these morphological abnormalities offers an effective bioindication of toxic stress in modern freshwater ecosystems^{34,35} and over previous time periods.^{36–38} The mentum and other mouthparts of chironomid larvae damaged during the cleaning and mounting process usually have abrupt breaks that are clearly visible and easily distinguishable from deformed structures.³⁹

The chironomid-based paleolimnological study was designed to track and compare past changes in incidence of larval mouthpart deformities in identical chironomid taxa from RAS and RPD. To provide background information on the structure of the subfossil chironomid assemblages, sediment core samples from both water bodies were analyzed for species composition of the assemblages following standard procedures outlined in Brooks et al.⁴⁰ (see SI 2 for more details). Larval head capsules of the two most common chironomid taxa, *Pseudodiames nivosa* and *Micropsectra radialis*-type, found in both dredge and sediment core samples (live specimens and their subfossil remains, respectively) from RAS and RPD (SI Figures S1 and S3) were inspected for deformities of the mentum, a mouth part which is typically well preserved in subfossil material.

Three biometric variables, head length, head width, and mentum width, were measured for each head capsule. These variables were used to assign each head capsule to a specific larval stage of development (instar). A minimum of 100 third- and fourth-instar head capsules of each of the two chironomid taxa, *P. nivosa*- and *M. radialis*-type, were inspected for mentum deformities in each sediment sample at 250–400× magnification using a compound microscope. The severity of mentum deformities was categorized into three classes according to Lenat:⁴¹ Class I—slight deformities, such as 'fused' teeth; Class II—more conspicuous, moderate deformities, such as extra teeth, missing teeth, large gaps, and distinct asymmetry; and Class III—severe deformities, including at least two Class II characteristics. Head capsules of live larvae were treated and inspected for mentum deformities in the same manner as their subfossil remains.

Statistical Analyses. One-way analysis of variance (ANOVA), followed by Bonferroni post hoc test, was used to determine whether there are any significant differences in the

Table 1. Physical and Chemical Properties of Water in RAS and RPD in the Early Open-Water Season^a

parameter ^b	RAS ^c		(n = 3)	EU limit value ^d
	0–5 m (n = 6)	5–9 m (n = 4)		
conductivity ($\mu\text{S cm}^{-1}$ at 25 °C)	231 ± 46 ^k	857 ± 117 ^m	47 ± 6 ⁿ	2500
total ions ($\mu\text{equiv}\cdot\text{L}^{-1}$)	4,185 ± 1169 ^k	18,513 ± 2938 ^m	779 ± 103 ⁿ	NA
Ca ²⁺ (mg L^{-1})	18 ± 6 ^k	76 ± 10 ^m	3 ± 1 ^k	NA
Mg ²⁺ (mg L^{-1})	13 ± 4 ^k	63 ± 10 ^m	0.7 ± 0.1 ⁿ	NA
Na ⁺ (mg L^{-1})	0.6 ± 0.1 ^k	4.0 ± 0.4 ^m	0.2 ± 0.1 ^k	200
K ⁺ (mg L^{-1})	0.3 ± 0.1 ^k	1.1 ± 0.1 ^m	0.2 ± 0.1 ^k	NA
SO ₄ ²⁻ (mg L^{-1})	99 ± 28 ^k	310 ± 124 ^m	15 ± 3 ⁿ	250
TP ^e ($\mu\text{g L}^{-1}$)	1.4 ± 0.1 ^k	1.6 ± 0.1 ^k	1.5 ± 0.5 ^k	NA
NO ₃ ⁻ -N ^f ($\mu\text{g L}^{-1}$)	191 ± 23 ^k	208 ± 14 ^k	172 ± 22 ^k	NA
NH ₄ ⁺ -N ^g ($\mu\text{g L}^{-1}$)	18 ± 5 ^{k,m}	35 ± 13 ^m	5 ± 1 ^k	NA
Al ($\mu\text{g L}^{-1}$)	395 ± 120 ^k	1,519 ± 126 ^m	3 ± 1 ⁿ	200
Cu ($\mu\text{g L}^{-1}$)	4 ± 1 ^k	9 ± 4 ^k	<2 ^m	2000
Fe ($\mu\text{g L}^{-1}$)	1 ± 1 ^{k,m}	7 ± 4 ^m	<1 ^k	200
Mn ($\mu\text{g L}^{-1}$)	181 ± 45 ^k	1,587 ± 609 ^m	<1 ⁿ	50
Ni ($\mu\text{g L}^{-1}$)	107 ± 32 ^k	468 ± 91 ^m	2 ± 2 ⁿ	20
Sr ($\mu\text{g L}^{-1}$)	72 ± 19 ^k	277 ± 37 ^m	14 ± 5 ⁿ	NA
Zn ($\mu\text{g L}^{-1}$)	85 ± 23 ^k	311 ± 29 ^m	3 ± 2 ⁿ	NA
pH	5.48 ± 0.11 ^k	5.07 ± 0.08 ^m	6.51 ± 0.14 ⁿ	≥6.5

^aRAS data for 2011–2012, and RPD data for 2010–2012. ^bFor each parameter, values (mean ± SE) that share common letters (k, m, or n) do not differ significantly (one-way ANOVA and Bonferroni post hoc test, $p < 0.05$). ^cValues are for the upper (0–5 m depth) and lower (5–9 m depth) parts of the RAS water column. ^dNA: not available, i.e. parameter is not regulated by the European Drinking Water Directive;⁴⁷ parameter values exceeding the appropriate European Union limit values for drinking water⁴⁷ are shown in bold. ^eTP = total phosphorus. ^fNO₃⁻-N = nitrate-nitrogen. ^gNH₄⁺-N = ammonium-nitrogen.

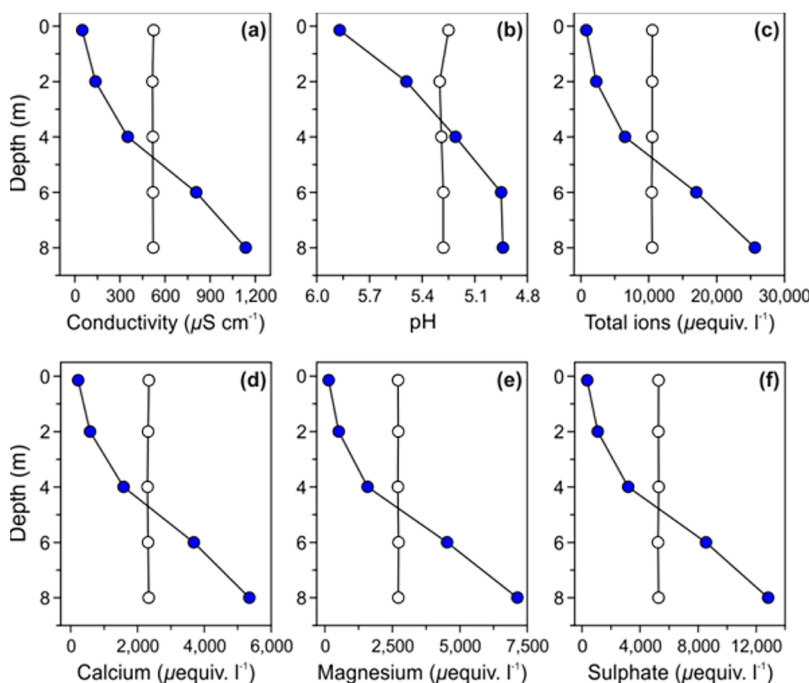


Figure 2. Depth profiles of selected physical and chemical properties of the RAS water. Electrical conductivity (a), pH (b), total ion (c), calcium (d), magnesium (e), and sulfate (f) profiles in the RAS water column on fourth July 2012 (closed circles; the lake was ~70% ice covered) and 29th August 2012 (open circles; ~1.5 months prior to lake ice freeze-up).

elemental composition of water, sediment, and biota between the two adjacent water bodies, as well as between the shallow and deep-water habitats of RAS. All data were square root transformed to reduce the biasing effect of extremely low or high element concentrations. The nonparametric Mann–Whitney U-test was used to detect significant differences in the frequency of chironomid deformities between different time intervals in the Holocene. Percentage data were transformed to

square roots to stabilize variances. SPSS version 17.0 software (SPSS Inc., Chicago, IL) was used.

RESULTS AND DISCUSSION

Water Chemistry. Chemical analysis of water samples revealed that the ratios of dissolved inorganic nitrogen (DIN = NO₃⁻-N + NH₄⁺-N) to total phosphorus (TP) exceed 100 by

mass in RAS and RPD (see SI 3 for more details). This suggests that phytoplankton communities in both water bodies are phosphorus-limited, defined by Bergström⁴² as DIN:TP > 3.4 by mass. Physico-chemical analysis of water taken from RAS and RPD in 2010–2012 indicated that the striking differences in limnochemistry of these two neighboring water bodies, recorded in 2005,¹⁸ persisted to the present day (Table 1). Although the water in both water bodies is dominated by the same ions (Ca^{2+} , Mg^{2+} , and SO_4^{2-}), the total ion concentration and electrical conductivity in RAS (~10 500 $\mu\text{equiv. L}^{-1}$ and ~510 $\mu\text{S cm}^{-1}$, respectively) are more than an order of magnitude greater than in RPD (~780 $\mu\text{equiv. L}^{-1}$ and ~45 $\mu\text{S cm}^{-1}$, respectively). The concentrations of many dissolved minor and trace elements (Al, Cu, Mn, Ni, Sr, Zn) are negligibly small (one-way ANOVA, Bonferroni post hoc test, $p < 0.05$) in the circumneutral RPD (pH 6.19–6.64) compared to the acidic RAS (pH 4.93–5.86) (Table 1). The concentrations of dissolved iron are extremely low (<10 $\mu\text{g L}^{-1}$) in both water bodies. However, in the acidic RAS, an extensive area of the lake bottom at 5.0–8.5 m water depth is coated with orange-colored iron oxyhydroxides (SI Figures S1). It is known that under mildly acidic conditions in surface waters affected by ARD, the soluble ferrous iron oxidizes to ferric iron, which precipitates as a ferric oxyhydroxide.⁴³

In the RAS catchment dominated by crystalline basement rocks with an inherently low acid buffering capacity, enhanced cryogenic weathering attributed to ice of the active rock glacier is the most likely mechanism causing groundwater inputs of acidic, metal- and sulfate-enriched water to the lake. Cryogenic weathering of the local bedrock, which involves a plethora of physical, chemical and biological processes (ice segregation, freeze–thaw cycles, volumetric expansion of water, hydration etc.),^{44–46} results in the exposure of fresh bedrock surfaces to air and water in a complex rock glacier system and leads to oxidation of sulfide minerals and the generation of ARD.

A solute-rich inflow sinks, as a rule, down the water column due to its high density. This effect can result in physical and chemical stratification of the water column which reduces water circulation and aeration of deep-water layers. Our data show that strong stratification develops in RAS during periods of prolonged ice cover (8–9 months). After the ice breakup, the concentrations of major ions (Ca^{2+} , Mg^{2+} , SO_4^{2-}) and minor and trace elements (Al, Mn, Ni, Sr, Zn) in the upper water layers (0–5 m) are four to seven times smaller than in the deeper waters (5–9 m), and the pH decreases from 5.48 near the surface to 5.07 at depth (Table 1 and Figure 2).

Thus, the short growing season in RAS begins under extremely unfavorable conditions for aquatic life, especially in the deep water, and the lake water may be dangerous for human consumption. In fact, the concentrations of manganese, nickel, aluminum, and sulfate in the deep water (5–9 m) exceed the appropriate EU limits for drinking water⁴⁷ 32, 23, 7, and 2 times, respectively (Table 1). Although solutes become more homogeneously distributed in the water column by late August/early September due to destratification by wind-induced mixing and convection (Figure 2), concentrations of manganese, nickel, and aluminum along a water depth gradient remain considerably higher (520–820, 140–220, and 440–620 $\mu\text{g L}^{-1}$, respectively) than the EU maximum permissible levels in drinking water.

Total metal concentration, however, does not necessarily correspond with metal bioavailability and toxicity to aquatic organisms.⁴⁸ The proportion of the total metal content that is

available for uptake by biota depends greatly on the chemical form in which the metals are present. Metals in aquatic systems can exist in different chemical forms, including the dissolved inorganic complexes with dissolved anions (e.g., hydroxides, sulfates, carbonates) where metals occur as free hydrated metal ions, organic complexes with dissolved organic matter, and variety of particulate forms incorporated into the matrix of solid organic or mineral particles.⁴⁸ The free ionic form of metals is the most relevant for uptake by biota and hence the most toxic to aquatic life.^{49,50} Hydrogen ion activity (pH) and redox potential greatly affect metal availability because of their strong influences on metal partitioning and speciation. Numerous studies have shown that the free metal ion concentrations increase with decreasing pH as well as upon oxidation of initially reduced environments.^{48,51,52}

Thus, both processes, namely winter stratification resulting in low pH in the deep waters (pH ~5.1), and oxygenation of the metal-rich hypolimnion and sediment during the open-water season, may result in greater bioavailability and toxicity of metals to biota in RAS.

Sediments and Biota. *Sediments.* The concentrations of most metals in the sediments of RAS and RPD are comparable with their abundances in the Earth's continental crust (Figure 3). Rather high concentrations of lead and zinc in sediments of both water bodies may be attributed to the site-specific geologic conditions, whereas elevated nickel and copper concentrations (244 and 179 $\mu\text{g g}^{-1}$, respectively) in the RAS deep-water sediments are likely to be caused by enhanced accumulation of fine-grained particles in the deep water. These particles provide a large surface area for the sorption of metals at the water-sediment interface.⁵³

Chironomids. Concentrations of 10 elements (Cu, Zn, Pb, Ni, Cr, Al, Fe, Ti, Mn, and V) were significantly higher (one-way ANOVA, Bonferroni post hoc test, $p < 0.05$) in the larvae of *Pseudodiamesia nivosa*, omnivores that feed on a wide variety of foods from detritus to small invertebrates,⁵⁴ collected from the RAS deep water than from RPD unaffected by the rock glacier solutes (Figure 3). This suggests a high bioavailability of these metals in the RAS deep-water habitats.

Aquatic Moss. The aquatic moss *Warnstorfia exannulata*, which prefers mildly acidic conditions,⁵⁵ have colonized an extensive area of the RAS bottom at 5–8 m water depth (SI Figures S1). Increased concentrations of nickel and aluminum in the *W. exannulata* tissues were comparable to those recorded in the chironomid larvae from the RAS deep-water habitats (Figure 3). Aquatic mosses are considered to be good indicators of metal contamination.⁵⁶ They are tolerant of metal contamination, long-lived, and have large cationic exchange properties within the cell wall. Owing to the lack of roots, metal uptake occurs straight from the water where they develop.

Oligochaetes. Among all benthic organisms analyzed from the RAS deep water, the highest concentrations of Cu, Zn, and Pb were recorded in the body tissues of the sediment-ingesting oligochaete *Tubifex tubifex* (one-way ANOVA, Bonferroni post hoc test, $p < 0.05$). The Cu concentrations in the *T. tubifex* tissues were ~2.5 times greater (one-way ANOVA, Bonferroni post hoc test, $p < 0.05$) than that in surrounding sediments (Figure 3). Ingestion of contaminated sediment has been shown to be the major source of particle-sorbed metals to sediment-feeding organisms.⁵⁷

Aquatic Beetles. The Cu concentrations in the predatory beetle *Agabus bipustulatus*, which is common in shallow-water

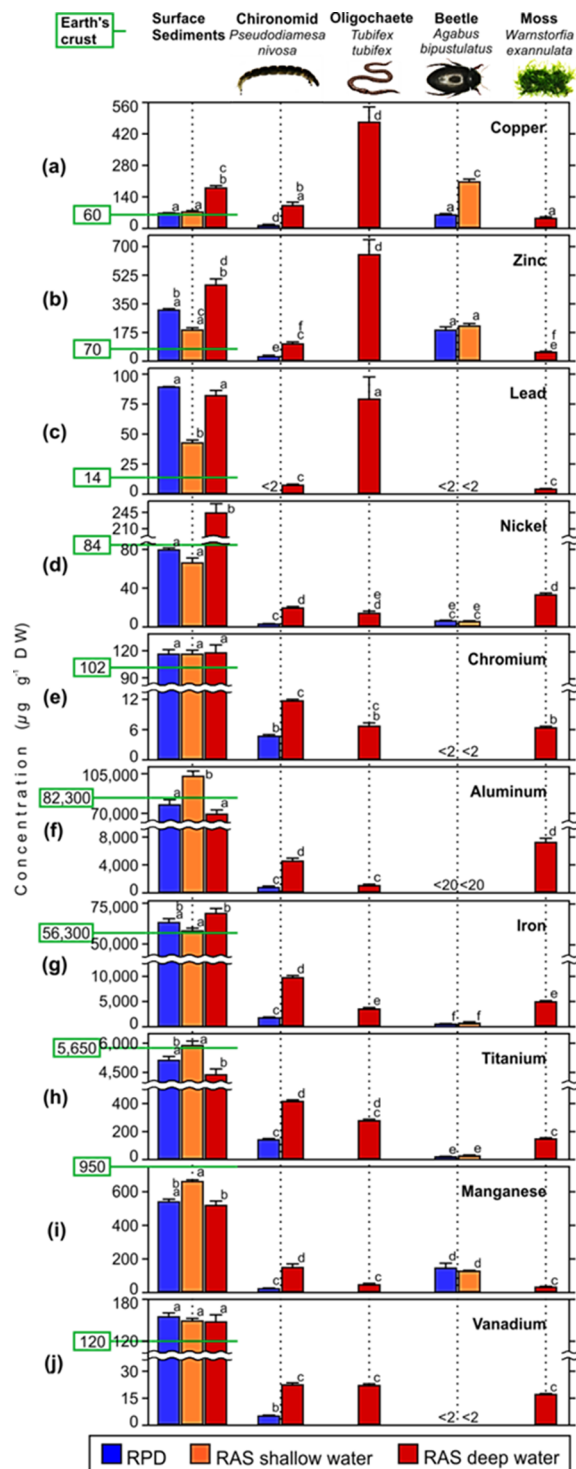


Figure 3. Concentrations (mean \pm SE; $n = 3$) of copper (a), zinc (b), lead (c), nickel (d), chromium (e), aluminum (f), iron (g), titanium (h), manganese (i), and vanadium (j) in surface sediments and biota of RPD and the RAS shallow and deep waters. For each metal, means followed by the same letter are not significantly different (one-way ANOVA, Bonferroni post hoc test, $p < 0.05$). The abundances of the chemical elements in the Earth's continental crust²² are shown with green lines.

habitats of both water bodies, were also significantly higher (one-way ANOVA, Bonferroni post hoc test, $p < 0.05$) in RAS than those from RPD (Figure 3). Results of a recent study⁵⁸ demonstrate that predatory aquatic beetles are capable of

reflecting trace elements bioaccumulation in habitats with different disturbance levels, although their innate ability to take up/excrete metals may vary widely between species.

Mentum Deformities in Modern Chironomid Larvae. Inspection of modern *Pseudodiamesa nivosa* and *Micropsectra radialis*-type larvae, represented by live specimens and their recent remains in surface sediments, for deformities of mentum revealed the morphological abnormalities in the RAS *P. nivosa* population. No mentum deformities were noted upon inspection of *P. nivosa* from RPD and *M. radialis*-type from both water bodies. Although mentum deformities in *Micropsectra* larvae have been recorded at some metal-contaminated sites,^{37,59} it is likely that the *P. nivosa* larvae are more susceptible to the harmful effects of acidic, metal-rich environments than the *M. radialis*-type larvae. Incidence of mentum deformities in the live *P. nivosa* larvae from RAS varied from 81% to 87% ($n = 3$) and was comparable with the frequency of mentum deformities among recent remains of *P. nivosa* in the RAS surface sediments (78–87%, $n = 3$). The observed deformities were categorized into two classes following Lenat.⁴¹ Class I—fused median tooth (30–34%, $n = 6$), and Class II—large median gap (48–55%, $n = 6$) or extra teeth (<2%, $n = 6$) (Figure 4). Mentum abnormalities are

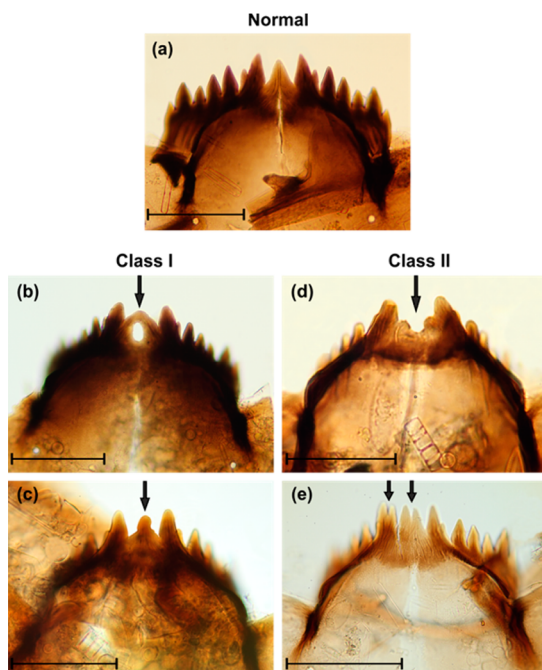


Figure 4. Micrographs (200 \times magnification) of larval menta of the chironomid *Pseudodiamesa nivosa* from the RAS modern and subfossil material: normal mentum (a) and deformed menta (b–e). The severity of the observed deformities was categorized into two classes following Lenat:⁴¹ Class I (slight deformities)—fused median tooth (b, c), and Class II (more conspicuous deformities)—large median gap (d) and extra teeth (e). Scale bars = 0.1 mm.

generally related to a physiological disturbance during the molting process, as a somatic response to a wide range of environmental stress factors, but not to a genetic heritability of larvae.^{60–62} In many polluted sites, the total incidence of deformities in chironomid populations usually varies between 20% and 50%,^{41,63} but the incidence of abnormalities in the RAS *P. nivosa* population (78–87%) was as high as that recorded in a population of *Chironomus* spp. (~83%), another

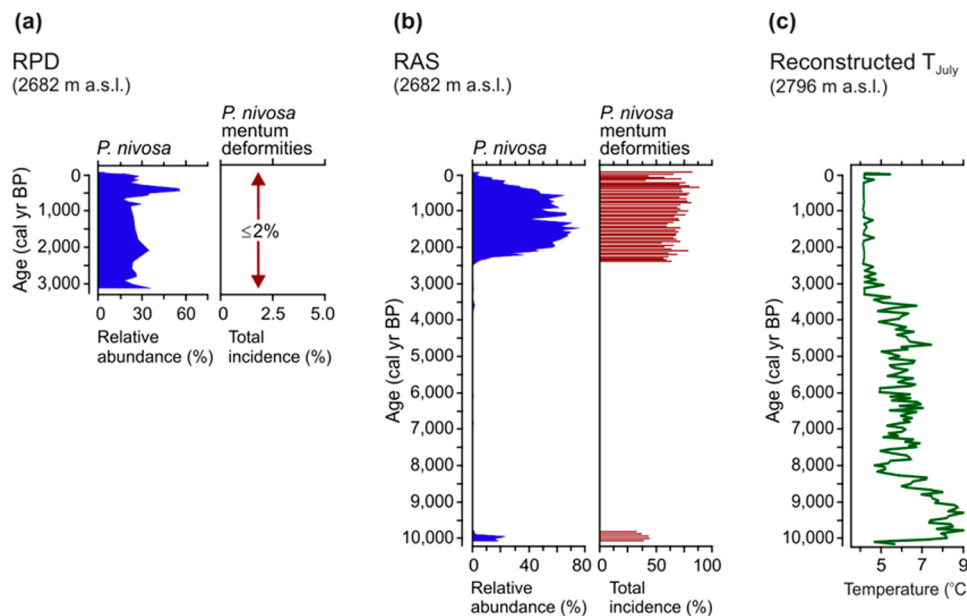


Figure 5. Relative abundance of *Pseudodiamesa nivosa* in chironomid assemblages and the total incidence of *P. nivosa* mentum deformities in the sediment records from RPD (a) and RAS (b), and Holocene July air temperatures (T_{July}) reconstructed for the Eastern Alps (c).⁶⁵

chironomid taxon, in a site heavily polluted by radionuclides and trace metals.⁶⁴

Reconstruction of Temporal Trends in the Ecotoxicological State. The analysis of chironomid remains in core sediment samples showed that a high total incidence of *P. nivosa* mentum deformities of ~70% persisted in RAS during the last 2.5 millennia and was significantly lower (Mann–Whitney U-test, $p < 0.0004$), around 40%, in the early Holocene (~10 150–9800 cal yr BP) (Figure 5). The incidence of the Class II mentum deformities (median gap or extra teeth) in *P. nivosa* from RAS was also significantly higher (Mann–Whitney U-test, $p < 0.0008$) in the late Holocene (~49%) than in the early Holocene (~21%). Unfortunately, the cold-stenothermal *P. nivosa* was absent in RAS, like other high alpine lakes,⁶⁵ through a relatively warm interval of the early and mid-Holocene (Figure 5, SI Figure S3), and this species cannot be used for reconstruction of temporal trends in the ecotoxicological state of RAS over the entire Holocene. In RPD, the frequency of *P. nivosa* mentum abnormalities did not exceed 2% (only the Class I mentum deformities was recorded) through the last 3.2 millennia, or, in other words, it did not exceed the frequency of chironomid deformities found in natural unstressed environments (up to 12–14%).^{41,66}

The results provide evidence that the present adverse conditions in the lake are not unprecedented in its Holocene history and cannot be associated exclusively with global warming and enhanced thawing of the rock glacier in recent years. It is likely that the development of the rock glacier started at the onset of the Holocene, when the area occupied by the modern rock glacier became deglaciated. The formation of RAS at the toe of the rock glacier most probably began at the onset of acidic drainage in the freshly deglaciated area.

Overall, our findings illustrate that natural ARD systems generated by active rock glaciers in mineralized areas with sulfide-bearing lithologies may seriously disturb lake ecosystems and endanger the quality of drinking water in pristine alpine environments. More adverse effects may be expected in lakes

situated at the toe of greater and more active rock glaciers than the one in the RAS catchment.

■ ASSOCIATED CONTENT

Supporting Information

More detailed descriptions of methods and results. This material is available free of charge via the Internet at <http://pubs.acs.org>.

■ AUTHOR INFORMATION

Corresponding Author

*Phone: +43 512 50751736; fax: +43 512 50751799; e-mail: boris.ilyashuk@uibk.ac.at.

Notes

The authors declare no competing financial interest.

■ ACKNOWLEDGMENTS

This work was funded by the Austrian Science Fund (FWF grant M1337-B17 to B.P.I.), the Melting Project of the Austrian Academy of Sciences (ÖAW grant to K.A.K.), and by the Nickel Control Project of the Autonomous Province Bolzano/Bozen (grant to K.A.K.). We appreciate technical assistance from Richard Niederreiter and Reinhard Lackner with field work and Josef Franzoi, Gry Larsen and Salvador Morales-Gomez with chemical analyses. We also would like to thank the three anonymous reviewers for helpful suggestions that improved this manuscript.

■ REFERENCES

- (1) Haeberli, W.; Hölzle, M. Application of inventory data for estimating characteristics of and regional climate-change effects on mountain glaciers: A pilot study with the European Alps. *Ann. Glaciol.* **1995**, *21*, 206–212.
- (2) Frauenfelder, R. *Regional-scale modelling of the occurrence and dynamics of rockglaciers and the distribution of paleopermafrost*. Ph.D. Dissertation, University of Zürich, Zürich, 2005.
- (3) Brown, G. H. Glacier meltwater hydrochemistry. *Appl. Geochem.* **2002**, *17*, 855–883.

- (4) Williams, M. W.; Knauf, M.; Caine, M.; Liu, F.; Verplanck, P. L. Geochemistry and source waters of rock glacier outflow, Colorado Front Range. *Permafrost Perigl. Process.* **2006**, *17*, 13–33.
- (5) Caine, N. Recent hydrologic change in a Colorado alpine basin: An indicator of permafrost thaw? *Ann. Glaciol.* **2010**, *51*, 130–134.
- (6) Sommaruga-Wögrath, S.; Koinig, K. A.; Schmidt, R.; Sommaruga, R.; Tessadri, R.; Psenner, R. Temperature effects on the acidity of remote alpine lakes. *Nature* **1997**, *387*, 64–67.
- (7) Slemmons, K. E. H.; Sarosa, J. E.; Simon, K. The influence of glacial meltwater on alpine aquatic ecosystems: A review. *Environ. Sci.: Processes Impacts* **2013**, *15*, 1794–1806.
- (8) Fortner, S. K.; Mark, B. G.; McKenzie, J. M.; Bury, J.; Trierweiler, A.; Baraer, M.; Burns, P. J.; Munk, L. Elevated stream trace and minor element concentrations in the foreland of receding tropical glaciers. *Appl. Geochem.* **2011**, *26*, 1792–1801.
- (9) Todd, A. S.; Manning, A. H.; Verplanck, P. L.; Crouch, C.; McKnight, D. M.; Dunham, R. Climate-change-driven deterioration of water quality in a mineralized watershed. *Environ. Sci. Technol.* **2012**, *46*, 9324–9332.
- (10) Runnels, D. D.; Shepherd, T. A.; Angino, E. E. Metals in water. Determining natural background concentrations in mineralized areas. *Environ. Sci. Technol.* **1992**, *26*, 2316–2323.
- (11) Nordstrom, D. K. Hydrogeochemical processes governing the origin, transport and fate of major and trace elements from mine wastes and mineralized rock to surface waters. *Appl. Geochem.* **2011**, *26*, 1777–1791.
- (12) Woo, M. K. *Permafrost Hydrology*; Springer-Verlag: Berlin, 2012.
- (13) Boeckli, L.; Brenning, A.; Gruber, S.; Noetzli, J. Permafrost distribution in the European Alps: Calculation and evaluation of an index map and summary statistics. *Cryosphere* **2012**, *6*, 807–820.
- (14) Barsch, D. *Rockglaciers: Indicators for the Present and Former Geocology in High Mountain Environments*; Springer-Verlag: Berlin, 1996.
- (15) Burger, K. C.; Degenhardt, J. J., Jr.; Giardino, J. R. Engineering geomorphology of rock glaciers. *Geomorphology* **1999**, *31*, 93–132.
- (16) Krainer, K.; Mostler, W. Hydrology of active rock glaciers: Examples from the Austrian Alps. *Arct., Antarct., Alp. Res.* **2002**, *34*, 142–149.
- (17) Vivioli, D.; Weingartner, R. The significance of mountains as sources of the world's fresh water. *GAIA* **2002**, *11*, 182–186.
- (18) Thies, H.; Nickus, U.; Mair, V.; Tessadri, R.; Tait, D.; Thaler, B.; Psenner, R. Unexpected response of high alpine lake waters to climate warming. *Environ. Sci. Technol.* **2007**, *41*, 7424–7429.
- (19) Psenner, R.; Schmidt, R. Climate-driven pH control of remote alpine lakes and effects of acid deposition. *Nature* **1992**, *356*, 781–783.
- (20) Tollmann, A. Geology and tectonics of the Eastern Alps (Middle Sector). *Abh. Geol. B.-A* **1980**, *34*, 197–255.
- (21) Sonnleitner, R.; Redl, B.; Schinner, F. Microbial mobilization of major and trace elements from catchment rock samples of a high mountain lake in the European Alps. *Arct., Antarct., Alp. Res.* **2011**, *43*, 465–473.
- (22) CRC Handbook of Chemistry and Physics, 85th ed.; Lide, D. R., Ed.; CRC Press: Boca Raton, FL, 2004.
- (23) Giardino, J. R., et al. 1992. A model of water movement in rock glaciers and associated water characteristics. In *Periglacial Geomorphology*; Dixon, J. C., Abrahams, A. D., Eds.; Wiley: Chichester, 1992; pp 159.
- (24) Leopold, M.; Williams, M.; Caine, N.; Völkel, J.; Dethier, D. Internal structure of the Green Lake 5 rock glacier, Colorado Front Range, USA. *Permafrost Periglacial Process.* **2011**, *22*, 107–119.
- (25) de Jong, R.; Kamenik, C.; Grosjean, M. Cold-season temperatures in the European Alps during the past millennium: Variability, seasonality and recent trends. *Quat. Sci. Rev.* **2013**, *82*, 1–12.
- (26) Monnier, S.; Kinnard, C. Internal structure and composition of a rock glacier in the Andes (upper Choapa valley, Chile) using borehole information and ground-penetrating radar. *Ann. Glaciol.* **2013**, *54*, 61–72.
- (27) Marion, G. M.; Farren, R. E. Mineral solubilities in the Na–K–Mg–Ca–Cl–SO₄–H₂O system: A re-evaluation of the sulphate chemistry in the Spencer–Møller–Weare model. *Geochim. Cosmochim. Acta* **1999**, *63*, 1305–1318.
- (28) Mosello, R.; Wathne, B. M. Surface water. Chemical analysis of major ions and nutrients. Analytical quality control. In *MOLAR: Measuring and Modelling the Dynamic Response of Remote Mountain Lake Ecosystem to Environmental Change: A Programme of Mountain Lake Research, MOLAR Project Manual*, NIVA Report 0-96061; NIVA; Wathne, B. M., Ed.; Oslo, 1997.
- (29) Boss, C. B.; Fredeen, K. J. *Concept, Instrumentation and Techniques in Inductively Coupled Plasma Optical Emission Spectrometry*, 2nd ed.; Perkin-Elmer: Norwalk, CT, 1997.
- (30) LaFleur, F. D., Ed. *Accuracy in Trace Analysis: Sampling, Sample Handling, Analysis*. Vol. 2. The United States Government Printing Office: Washington, DC, 1976.
- (31) Brown, C. L.; Luoma, S. N. Use of the euryhaline bivalve *Potamocorbula amurensis* as a biosentinel species to assess trace metal contamination in San Francisco Bay. *Mar. Ecol.: Prog. Ser.* **1995**, *124*, 129–142.
- (32) Kingston, H. M.; Jassie, L. B., Eds. *Introduction to Microwave Sample Preparation: Theory and Practice*; ACS: Washington, DC, 1988.
- (33) Bronk Ramsey, C. Radiocarbon calibration and analysis of stratigraphy: The OxCal program. *Radiocarbon* **1995**, *37*, 425–430.
- (34) Vermeulen, A. C. Elaborating chironomid deformities as bioindicators of toxic sediment stress: The potential application of mixture toxicity concepts. *Ann. Zool. Fenn.* **1995**, *32*, 265–285.
- (35) Warwick, W. F. Morphological abnormalities in Chironomidae (Diptera) larvae as measures of toxic stress in freshwater ecosystems: Indexing antennal deformities in *Chironomus* Meigen. *Can. J. Fish. Aquat. Sci.* **1985**, *42*, 1881–1914.
- (36) Warwick, W. F. Paleolimnology of the Bay of Quinte, Lake Ontario: 2800 years of cultural influence. *Can. Bull. Fish. Aquat. Sci.* **1980**, *206*, 1–117.
- (37) Wiederholm, T. Incidence of deformed chironomid larvae (Diptera: Chironomidae) in Swedish lakes. *Hydrobiologia* **1984**, *109*, 243–249.
- (38) Ilyashuk, B.; Ilyashuk, E.; Dauvalter, V. Chironomid responses to long-term metal contamination: A paleolimnological study in two bays of Lake Imandra, Kola Peninsula, northern Russia. *J. Paleolimnol.* **2003**, *30*, 217–230.
- (39) Dermott, R. M. Deformities in larval *Procladius* sp. and dominant Chironomini from the St. Clair River. *Hydrobiologia* **1991**, *219*, 171–185.
- (40) Brooks, S. J.; Langdon, P. G.; Heiri, O. *The Identification and Use of Palaeartic Chironomidae Larvae in Palaeoecology*; Quaternary Research Association: London, 2007.
- (41) Lenat, D. R. Menthum deformities of *Chironomus* larvae to evaluate the effects of toxicity and organic loading in streams. *J. N. Am. Benthol. Soc.* **1993**, *12*, 265–269.
- (42) Bergström, A.-K. The use of TN:TP and DIN:TP ratios as indicators for phytoplankton nutrient limitation in oligotrophic lakes affected by N deposition. *Aquat. Sci.* **2010**, *72*, 277–281.
- (43) Stumm, W.; Morgan, J. J. *Aquatic Chemistry: Chemical Equilibria and Rates in Natural Waters*, 3rd ed.; John Wiley & Sons: New York, NY, 1996.
- (44) Hall, K. Freeze-thaw weathering: The cold region 'Panacea'. *Polar Geogr. Geol.* **1995**, *19*, 79–87.
- (45) Hall, K.; Thorn, C. E.; Matsuoka, N.; Prick, A. Weathering in cold regions: Some thoughts and perspectives. *Prog. Phys. Geog.* **2002**, *26*, 577–603.
- (46) Murton, J. B.; Peterson, R.; Ozouf, J.-C. Bedrock fracture by ice segregation in cold regions. *Science* **2006**, *314*, 1127–1129.
- (47) The EU Council Directive 98/83/EC of 3 November 1998 on the quality of water intended for human consumption. *Off. J. Eur. Comm.* 1998, L330.
- (48) Luoma, S. N. Bioavailability of trace metals to aquatic organisms – a review. *Sci. Total Environ.* **1983**, *28*, 1–22.

- (49) Hare, L.; Tessier, A. Predicting animal cadmium concentrations in lakes. *Nature* **1996**, *380*, 430–432.
- (50) Di Toro, D. M.; Allen, H. E.; Bergman, H. L.; Meyer, J. S.; Paquin, P. R.; Santore, R. C. Biotic ligand model of the acute toxicity of metals. 1. Technical basis. *Environ. Toxicol. Chem.* **2001**, *20*, 2383–2396.
- (51) Du Laing, G.; Rinklebe, J.; Vandecasteele, B.; Meers, E.; Tack, F. M. G. Trace metal behaviour in estuarine and riverine floodplain soils and sediments: A review. *Sci. Total Environ.* **2009**, *407*, 3972–3985.
- (52) De Jonge, M.; Teuchies, J.; Meire, P.; Blust, R.; Bervoets, L. The impact of increased oxygen conditions on metal-contaminated sediments part I: Effects on redox status, sediment geochemistry and metal bioavailability. *Water Res.* **2012**, *46*, 2205–2214.
- (53) Hart, B. T. Uptake of trace metals by sediments and suspended particulates: A review. *Hydrobiologia* **1982**, *91*, 299–313.
- (54) Pagast, F. Systematik und Verbreitung der um die Gattung *Diaamesa* gruppieren Chironomiden. *Arch. Hydrobiol.* **1947**, *41*, 435–596.
- (55) Štechová, T.; Hájek, M.; Hájková, P.; Navrátilová, J. Comparison of habitat requirements of the mosses *Hamatocaulis vernicosus*, *Scorpidium cossinii* and *Warnstorffia exannulata* in different parts of temperate Europe. *Preslia* **2008**, *80*, 399–410.
- (56) Zechmeister, H. G.; et al. Bryophytes. In *Trace Metals and other Contaminants in the Environment. Vol. 6. Bioindicators and Biomonitoring: Principles, Concepts and Applications*; Markert, B. A., Breure, A. M., Zechmeister, H. G., Eds.; Elsevier: Amsterdam, 2003; pp 329.
- (57) Lee, B.-G.; Griscom, S. B.; Lee, J.-S.; Choi, H. J.; Koh, C.-H.; Luoma, S. N.; Fisher, N. S. Influences of dietary uptake and reactive sulfides on metal bioavailability from aquatic sediments. *Science* **2000**, *287*, 282–284.
- (58) Burghela, C. I.; Zaharescu, D. G.; Hoodac, P. S.; Palanca-Solera, A. Predatory aquatic beetles, suitable trace elements bioindicators. *J. Environ. Monit.* **2011**, *13*, 1308–1315.
- (59) Greijdanus-Klaas, M. Description of antennal deformation in larvae of *Micropsectra* (Kieffer) (Diptera; Chironomidae) from the river Rhine, The Netherlands. *Lauterbornia* **1993**, *14*, 17–22.
- (60) Groenendijk, D.; Zenstra, L. W. M.; Postma, J. F. Fluctuating asymmetry and mentum gaps in populations of the midge *Chironomus riparius* (Diptera: Chironomidae) from a metal-contaminated river. *Environ. Toxicol. Chem.* **1998**, *17*, 1999–2005.
- (61) Vermeulen, A. C.; Liberloo, G.; Ollevier, F.; Goddeeris, B. Ontogenesis, transfer and repair of mouthpart deformities during moulting in *Chironomus riparius* (Diptera, Chironomidae). *Arch. Hydrobiol.* **2000**, *147*, 401–415.
- (62) Meregalli, G.; Bettinetti, R.; Pluymers, L.; Vermeulen, A. C.; Rossaro, B.; Ollevier, F. Mouthpart deformities and nucleolus activity in field-collected *Chironomus riparius* larvae. *Arch. Environ. Contam. Toxicol.* **2002**, *42*, 405–409.
- (63) Wise, R. R.; Pierstorff, C. A.; Nelson, S. L.; Bursek, R. M.; Plude, J. L.; McNello, M.; Hein, J. Morphological deformities in *Chironomus* (Chironomidae: Diptera) larvae as indicators of pollution in Lake Winnebago, Wisconsin. *J. Great Lakes Res.* **2001**, *27*, 503–509.
- (64) Warwick, W. F.; Fitchko, J.; McKee, P. M.; Hart, D. R.; Burt, A. J. The incidence of deformities in *Chironomus* spp. from Port Hepe Harbour, Lake Ontario. *J. Great Lakes Res.* **1987**, *13*, 88–92.
- (65) Ilyashuk, E. A.; Koinig, K. A.; Heiri, O.; Ilyashuk, B. P.; Psenner, R. Holocene temperature variations at a high-altitude site in the Eastern Alps: A chironomid record from Schwarzsee ob Sölden, Austria. *Quat. Sci. Rev.* **2011**, *30*, 176–191.
- (66) Warwick, W. F. Morphological deformities in Chironomidae (Diptera) larvae as biological indicators of toxic stress. In *Toxic Contaminants and Ecosystem Health: A Great Lakes Focus*; Evans, M. S., Ed.; John Wiley & Sons: New York, NY, 1988.